Critical Role of the Programmed Death-1 (PD-1) Pathway in Regulation of Experimental Autoimmune Encephalomyelitis

Alan D. Salama,[1,3] Tanuja Chitnis,[2,3] Jaime Imitola,[2,3] Hisaya Akiba,[4] Fumihiko Tushima,[5] Miyuki Azuma,[5] Hideo Yagita,[4] Mohamed H. Sayegh,[1,3] and Samia J. Khoury[2]

[1]*Laboratory of Immunogenetics and Transplantation,* [2]*Centre for Neurologic Diseases, Brigham and Women's Hospital, and* [3]*Division of Nephrology, Children's Hospital, Harvard Medical School, Boston, MA 02115*
[4]*Department of Immunology, Juntendo University School of Medicine, Tokyo 113-8421, Japan*
[5]*Department of Molecular Immunology, Tokyo Medical and Dental University, Tokyo 113-8549, Japan*

Abstract

Experimental autoimmune encephalomyelitis (EAE) is mediated by autoantigen-specific T cells dependent on critical costimulatory signals for their full activation and regulation. We report that the programmed death-1 (PD-1) costimulatory pathway plays a critical role in regulating peripheral tolerance in murine EAE and appears to be a major contributor to the resistance of disease induction in CD28-deficient mice. After immunization with myelin oligodendrocyte glycoprotein (MOG) there was a progressive increase in expression of PD-1 and its ligand PD-L1 but not PD-L2 within the central nervous system (CNS) of mice with EAE, peaking after 3 wk. In both wild-type (WT) and CD28-deficient mice, PD-1 blockade resulted in accelerated and more severe disease with increased CNS lymphocyte infiltration. Worsening of disease after PD-1 blockade was associated with a heightened autoimmune response to MOG, manifested by increased frequency of interferon γ–producing T cells, increased delayed-type hypersensitivity responses, and higher serum levels of anti-MOG antibody. In vivo blockade of PD-1 resulted in increased antigen-specific T cell expansion, activation, and cytokine production. Interestingly, PD-L2 but not PD-L1 blockade in WT animals also resulted in disease augmentation. Our data are the first demonstration that the PD-1 pathway plays a critical role in regulating EAE.

Key words: costimulation • T cell • autoimmunity • tolerance • EAE

Introduction

Murine experimental autoimmune encephalomyelitis (EAE)* is a T cell–dependent disease model used to investigate the pathophysiology of multiple sclerosis. In this model, antigen-specific $CD4^+$ Th1 cells mediate inflammatory damage in the central nervous system (CNS), with consequent demyelination, manifested clinically by progressive paralysis (1). In addition to reacting with peptides derived from myelin constituents, these encephalitogenic T cells require the delivery of positive secondary costimulatory signals for their complete activation and generation of effector function (2–4).

In general, T cells are regulated by a number of nonmutually exclusive mechanisms, including clonal deletion mediated by apoptosis, anergy, and/or by soluble factors such as cytokines or by professional regulatory cells (5). Furthermore, negative signals delivered to activated T cells by regulatory costimulatory pathways are essential contributors to these mechanisms, and therefore act as natural inhibitors for effector T cell expansion (6). The prototypic molecule in this class is cytotoxic T lymphocyte–associated antigen 4 (CTLA-4), expressed on T cells after their activation. Blockade or deficiency of CTLA-4 leads to enhanced autoimmunity with augmentation of EAE (7). However, the B7 ligands that bind CTLA-4 also serve to mediate positive signals to the T cells through the ligation of CD28, which has made it harder to capitalize on a therapeutic strategy for the treatment of clinical disease by manipulating CTLA-4

Address correspondence to Samia J. Khoury, 77 Avenue Louis Pasteur, Room 714, Centre for Neurologic Diseases, Brigham and Women's Hospital, Boston, MA 02115. Phone: 617-525-5370; Fax: 617-525-5252; E-mail: skhoury@rics.bwh.harvard.edu

*Abbreviations used in this paper: ANOVA, analysis of variance; CNS, central nervous system; CTLA-4, cytotoxic T lymphocyte–associated antigen 4; DTH, delayed-type hypersensitivity; EAE, experimental autoimmune encephalomyelitis; GFAP, glial fibrillar-associated protein; MOG, myelin oligodendrocyte glycoprotein; PD-1, programmed death-1.

J. Exp. Med. © The Rockefeller University Press • 0022-1007/2003/07/71/8 $8.00
Volume 198, Number 1, July 7, 2003 71–78
http://www.jem.org/cgi/doi/10.1084/jem.20022119

signaling. Recently, a novel negative regulatory molecule and a new member of the B7-CD28 superfamily has been described, termed programmed death-1 (PD-1; 8). This molecule is found on activated $CD4^+$ and $CD8^+$ T cells, and binds to two known ligands, PD-L1 (also termed B7-H1) and PD-L2 (also termed B7-DC), found on APCs as well as on diverse parenchymal cell types (9–11). Ligation of the PD-1 receptor leads to diminished proliferation and IL-2 production, and induction of cell cycle arrest with $CD8^+$ T cells appearing to be more sensitive to this effect than $CD4^+$ cells (12). PD-1–deficient animals develop diverse autoimmune conditions, such as autoimmune cardiomyopathy (BALB/c background) and a lupus-like syndrome with arthritis and nephritis (C57BL/6 background; 13, 14). It is interesting that the precise autoimmune phenotype that develops is dependent on the genetic background of the animal in which the deficiency is produced. The development of an autoimmune phenotype in the absence of PD-1, reminiscent of that of CTLA-4–deficient animals (15) though less severe, led to the suggestion that this pathway may play a central role in the maintenance of peripheral tolerance toward autoantigens (16). Indeed, the parenchymal expression of PD-1 ligands may play a critical role in regulating autoimmune responses in various target organs. In this study, we used blocking antibodies to PD-1, PD-L1, and PD-L2 to investigate whether this pathway plays a role in the regulation of EAE. Our data confirm the important role of this costimulatory pathway in limiting inflammatory disease in EAE, which appears to exert an effect on both $CD4^+$ and $CD8^+$ cells and crucially plays a role in the resistance of disease induction in CD28-deficient animals. These data provide the rationale for developing a strategy for PD-1 ligation as a therapy to limit disease in EAE and multiple sclerosis.

Materials and Methods

Mice. Female WT or CD28-deficient C57BL/6 mice, and WT or DO-11.10 TCR transgenic BALB/c mice were purchased from The Jackson Laboratory and housed according to local and National Institutes of Health (NIH) guidelines. All mice were used at 6–8 wk of age.

EAE Induction with Myelin Oligodendrocyte Glycoprotein (MOG). MOG peptide 35–55 (MEVGWYRSPFSROVHLYRNGK) corresponding to the murine sequence was synthesized and HPLC purified by Quality Controlled Biochemicals. WT or CD28-deficient C57BL/6 mice were immunized subcutaneously in the flank with 200 μg MOG peptide in CFA (Sigma-Aldrich) and injected intraperitoneally with 200 ng pertussis toxin (List Biological Laboratories Inc.) on the day of immunization and 2 d later. EAE was scored as previously described (17) with a grade between 0 (no disease) and 5 (death).

Antibodies. The anti–mouse PD-1 mAb (J43, hamster IgG) has been described (8). The anti–mouse PD-L1 mAb (MIH6, rat IgG2a) and the anti–mouse PD-L2 mAb (TY25, rat IgG2a) were also recently described (18). Specific binding of these antibodies to their respective ligands has been demonstrated (19). Antibodies were manufactured by Bioexpres Cell Culture Inc. and given intraperitoneally according to the following regimen: 500 μg on the day of immunization and 250 μg on alternate days until day 10 after immunization. Delayed therapy consisted of the same dose regimen but was administered from day 10 after immunization. Control hamster IgG (ICN Pharmaceuticals Inc.) and control rat IgG (Sigma-Aldrich) were given according to the same protocol.

ELISPOT Analysis to Measure the Frequencies of MOG-reactive T Cells. The ELISPOT assay was adapted to measure IFN-γ–secreting cells. ELISAspot plates (Cellular Technology Limited) were coated with a capture antibody against IFN-γ (clone R4-6A2; BD Biosciences) in PBS and left overnight at 4°C. The plates were blocked with 1% BSA-PBS for 1 h and then washed with PBS. Between 5 and 10×10^5 splenocytes were added to each well in 100 μl RPMI 1640 medium containing 10% fetal calf serum (Sigma-Aldrich), 2 mM L-glutamine, 100 U/ml penicillin/streptomycin (BioWhittaker), and 50 μM 2-mercaptoethanol (Sigma-Aldrich). Control wells contained responder splenocytes plus medium alone. Cells were also tested in triplicate wells against concanavalin A (Sigma-Aldrich) and different concentrations of MOG peptide. After 48 h, the plates were washed and a biotinylated detection antibody (clone XMG1.2; BD Biosciences) was added and the plates were left for overnight incubation at 4°C. After further washing, horse radish peroxidase–conjugated avidin (DakoCytomation) was added for 2 h at room temperature. Development was with AEC (Sigma-Aldrich). The resulting spots were counted on a computer-assisted ELISASpot Image Analyzer (Cellular Technology Limited). The frequencies were then expressed as cytokine-producing cells per million splenocytes.

Histology. Spinal cords and brains were harvested on days 14–21 after immunization and snap frozen in optimal cutting temperature compound. 4–10-μm thick sections were cut, fixed in acetone, stained using the avidin-biotin technique (Vector Laboratories), and counterstained with hematoxylin. Antibodies used were anti-CD4 (clone H129.19), anti-CD8 (clone 53-6.7; BD Biosciences), anti-F4/80 (clone CI:A3-1; Caltag Laboratories), anti–PD-1 (J43), anti–PD-L1 (MIH6), and anti–PD-L2 (TY25). Isotype-matched control IgG and omission of the primary antibody served as negative controls. Each specimen was evaluated at three different levels of sectioning.

For dual staining of resident CNS cells, spinal cords were sectioned at 20 microns and incubated with anti–PD-L1, anti–PD-L2, anti–glial fibrillar-associated protein (GFAP; cocktail of clones 4A11, 1B4, and 2E1; BD Biosciences), and FITC-conjugated isolectin IB4 (LB4, from Griffonia simplicifolia; Molecular Probes) for 12 h. Sections were washed and incubated with appropriate fluorochrome-conjugated secondary antibodies, Alexa 488 (green) or Alexa 594 (red; Molecular Probes). Sections were analyzed using an immunofluorescence microscope equipped with image analysis systems.

Adoptive Transfer of DO11.10 TCR Transgenic T Cells and Anti-OVA Response. To investigate the effect of PD-1 blockade on antigen-specific T cells, adoptive transfer of OVA-specific DO11.10 TCR transgenic T cells was performed as previously described (6, 20, 21). In brief, splenocytes from DO11.10 mice containing 3×10^6 $CD4^+$ $KJ1\text{-}26^+$ T cells were injected intravenously into nonirradiated BALB/c mice. 24 h later, 100 μg $OVA_{323–339}$ peptide in IFA was injected subcutaneously. 4 d later, the animals were killed and the draining lymph nodes were collected. The extent of expansion of the $CD4^+$ $KJ1\text{-}26^+$ population was compared in animals treated with no OVA challenge, those immunized with OVA and receiving control hamster IgG, and those receiving immunization and anti–PD-1 mAb. Two to three mice were used in each group per experiment. Results are expressed as the absolute number of $CD4^+$ $KJ1\text{-}26^+$ cells for one representative experiment. Furthermore, isolated lymphocytes were incubated in vitro with 1 μg/ml $OVA_{323–339}$ peptide for 72 h,

and then stained for intracellular cytokine expression and activation markers. Results are expressed as the number of $CD4^+$ $KJ1\text{-}26^+$ cells expressing the markers.

Flow Cytometry. Splenocytes or lymph node cells were stained with antibodies to the activation marker CD25 and intracellular cytokines (IFN-γ, IL-4, IL-5, and IL-10; BD Biosciences). Cells were analyzed on a FACSCalibur™ (Becton Dickinson) using CELLQuest™ software (Becton Dickinson).

Measurement of Delayed-type Hypersensitivity (DTH) and Anti-MOG Antibodies. In each group, three to five animals were used at day 14 after immunization for measurement of DTH reactions and measurement of serum anti-MOG antibodies. DTH was assessed by measurement of the thickness of the footpad or ear, followed by intradermal injection on one side of MOG peptide (50 μg in 50 μl PBS) or on the contralateral side with an equal volume of PBS. After 48 h the change in skin thickness was measured and the net increase (with MOG peptide − control PBS) was calculated. Anti-MOG antibodies were measured by ELISA as previously reported (17) and their titre was expressed as the absorbance at 450 nm.

Results

PD-1 and PD-L1 Expression Is Increased over Time in the CNS of Animals with EAE. Animals with EAE were killed at different time points up to 1 mo from the time of immunization. Sections of their spinal cords were stained for PD-1 and its ligands PD-L1 and PD-L2. Staining revealed an increased level of PD-1 expression on infiltrating cells beginning in the second week, peaking at the third week, and persisting for the 4 wk studied (Fig. 1 a). Expression of PD-L1 increased over a similar time period, although we found no PD-L2 staining in the brains until day 30 when only minimal staining was observed (Fig. 1 a). This time course of expression of both PD-1 and PD-L1 closely follows that of clinical disease in mice with EAE: peaking in the second to third weeks (Fig. 2 a). Furthermore, using dual color staining we demonstrated PD-L1 but not PD-L2 expression on resident astrocytes (colocalized with anti-GFAP mAb) and microglial cells (colocalized with lectin IB4), in brains of animals with EAE at 20 and 30 d, respectively (Fig. 1 b).

Blockade of PD-1 Results in Accelerated and More Severe Disease in WT Mice. After in vivo blockade using anti–PD-1 mAb, a more rapid and higher grade disease was observed in animals immunized with MOG 33–55 peptide (Fig. 2 a). Compared with control animals treated with either control hamster IgG or carrier (PBS), there was a statistically significant increase in disease scores in the anti–PD-1 mAb-treated WT animals (mean maximal score 2.94 ± 1.3 vs. 1.75 ± 1.0 in control animals, $P = 0.005$ by two-tailed Mann-Whitney U test). Overall disease incidence

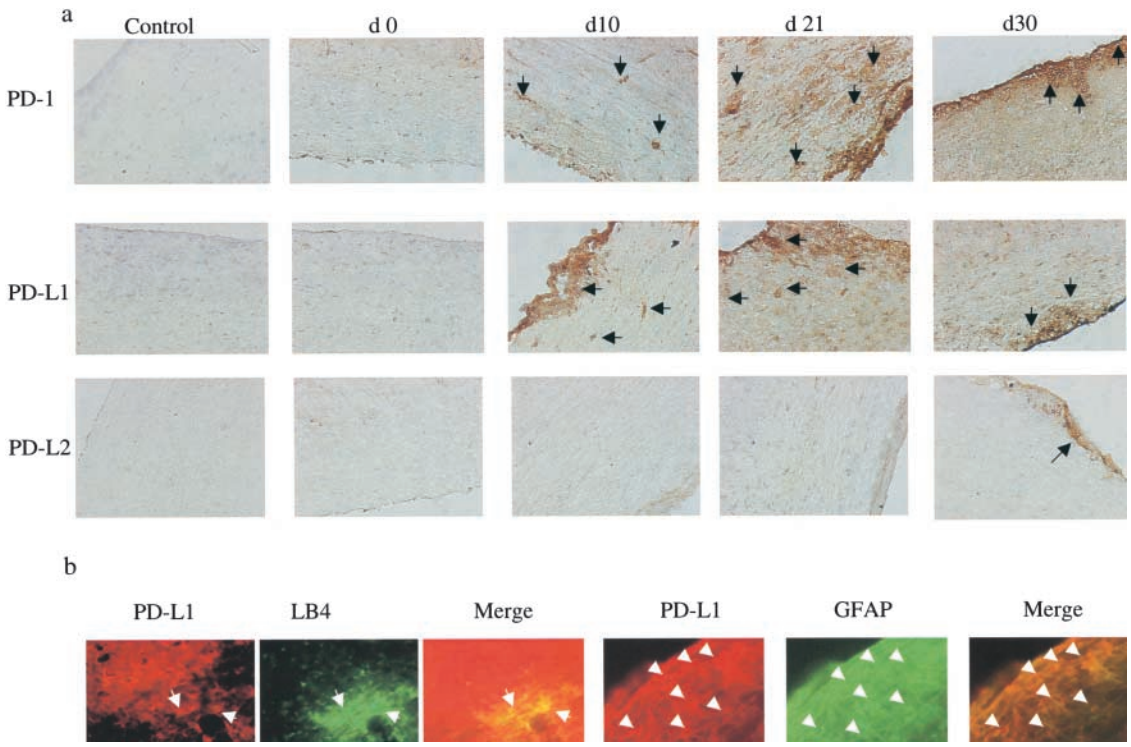

Figure 1. Expression of PD-1, PD-L1, and PD-L2 in the CNS of mice with EAE. (a) Time course of expression of PD-1, PD-L1, and PD-L2. Immunohistochemistry for PD-1, PD-L1, and PD-L2 expression in spinal cord sections from animals with EAE at different time points after immunization for up to 1 mo. The numbers above each plate represent the time after immunization when the animals were killed and the sections were stained. There is a progressive increase in the PD-1 and PD-L1 expression, which appears to peak by day 21 and begin to decline thereafter, mirroring the clinical tempo of disease (×100), whereas there is no PD-L2 staining until day 30 when it appears minimally. (b) Expression of PD-L1 on resident brain cells during EAE. Confocal immunohistochemistry demonstrating expression of PD-L1 on astrocytes (costained with GFAP on day 20 of EAE) and microglia (costained with lectin IB4 on day 30 of EAE; all ×40). No expression of PD-L2 was found on resident brain cells.

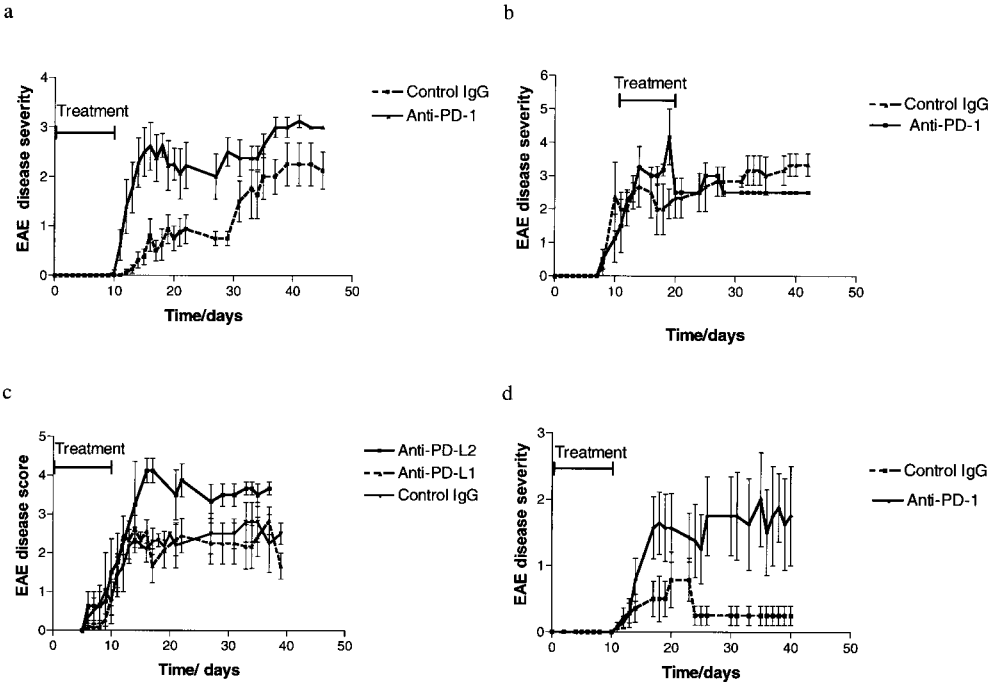

Figure 2. EAE outcome in animals treated with PD-1 pathway blockade. The disease scores for control and anti–PD-1–treated animals >40 d of follow up are shown, for WT mice with early therapy (a) and delayed therapy (b), and for CD28-deficient mice (d). There is a highly significant difference in disease severity between the early therapy and control groups ($P = 0.0053$ for WT and $P = 0.0074$ for CD28-deficient mice by two-tailed Mann-Whitney U test). No difference was found with delayed therapy. PD-L2 blockade also augmented disease ($P = 0.03$ compared with control by two-tailed Mann-Whitney U test) whereas PD-L1 blockade had no effect (c).

was similar in both groups (89%), although the PD-1 blockade group had an earlier onset compared with control, so that at 13 d after immunization the PD-1 blockade group had an incidence of 89% whereas the control group only had 25% incidence ($P = 0.0075$, $\chi 2$ test). By contrast, the delayed PD-1 blockade (beginning 10 d after immunization and continuing for 10 d) demonstrated no augmentation of disease compared with control Ig–treated animals (Fig. 2 b).

Blockade of PD-L2 but not PD-L1 Results in More Severe Disease in WT Mice. We then sought to examine the effects of blockade of the PD-1 ligands, PD-L1 or PD-L2, on disease course. In vivo administration of anti–PD-L2 mAb in WT mice resulted in disease augmentation compared with control Ig–treated animals (mean maximal score 4.125 ± 0.27 vs. 2.64 ± 0.5 in controls, $P = 0.030$ by two-tailed Mann-Whitney U test), although the overall incidence and time of onset were similar in the two groups (Fig. 2 c). By contrast, administration of anti–PD-L1 mAb had no effect on disease severity compared with controls (Fig. 2 c).

CD28-deficient Mice Are Protected from Disease Induction, but Lose Their Disease Resistance after PD-1 Blockade. We and others have previously reported that CD28-deficient mice are resistant to disease induction (3, 22) but are capable of developing disease after a more potent immune stimulus, such as double immunization or after CTLA-4/B7 blockade (3). After the PD-1 pathway blockade, CD28-deficient mice developed moderately severe disease (mean maximal disease score 2.07 ± 0.43 compared with 0.85 ± 0.37 in the control CD28-deficient group, $P = 0.0006$ by two-tailed Mann-Whitney U test; Fig. 2 d). The cumulative incidence and time of onset in the PD-1 blockade and control groups were similar. These data demonstrate that the disease resistance in CD28-deficient animals is related in part to inhibitory signaling through PD-1. Moreover, it is interesting to note that the mean disease score achieved with PD-1 blockade was greater than that achieved by CTLA-4 blockade previously reported by our group (3).

PD-1 Blockade Results in Increased Frequency of IFN-γ–producing MOG-reactive T Cells and DTH Responses. 14 d after MOG immunization, splenocytes were isolated from animals in each of the treatment groups and were assayed by ELISPOT for IFN-γ production in response to MOG peptide. When compared with the control animals, those treated with PD-1 blockade had a higher frequency of IFN-γ–producing MOG-reactive T cells in both WT (Fig. 3 a; $P = 0.017$ by one-way analysis of variance [ANOVA]) and CD28-deficient animals (Fig. 3 b; $P = 0.0254$ by one-way ANOVA). Moreover, in WT mice there was a significant increase in DTH reaction in the animals treated with anti–PD-1 mAb compared with controls (Fig. 3 c; $P = 0.0245$ by two-tailed Mann-Whitney U test).

PD-1 Blockade Increases anti-MOG Antibody Production. Because PD-1 is also up-regulated on activated B cells (8) and antigen-specific class-switched antibody production is a T cell–dependent process, we measured anti-MOG IgG antibody production in animals treated with anti–PD-1 mAb or control IgG. 14 d after immunization, serum was obtained from the animals and anti-MOG antibodies were measured by ELISA. In both WT and CD28-deficient animals there was a significant increase in the level of anti-MOG antibodies measured after the PD-1 blockade (Fig. 3 d).

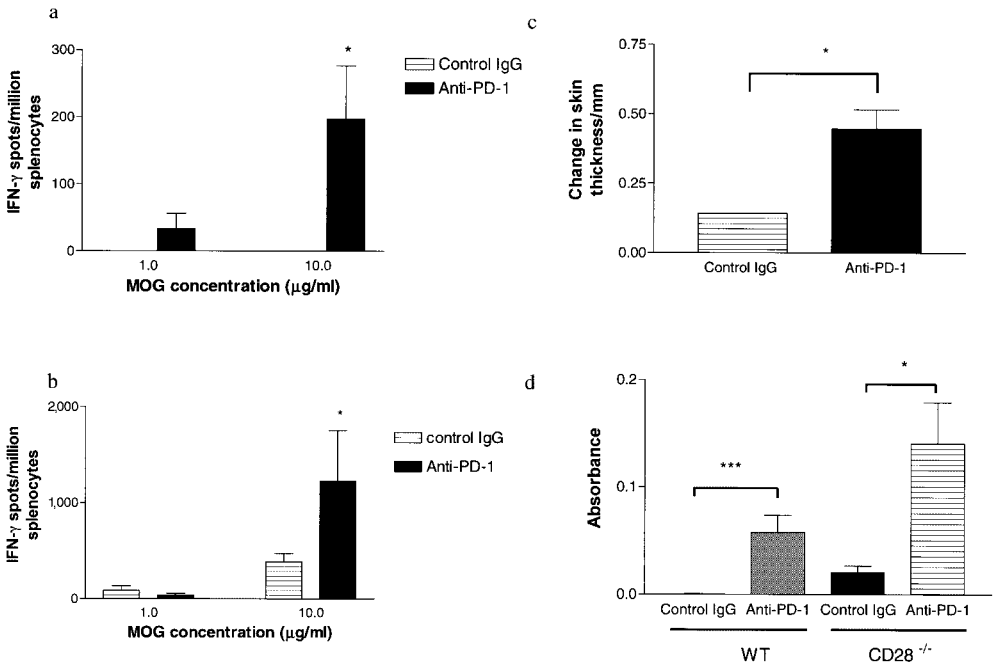

Figure 3. T cell and antibody responses to MOG in animals treated with PD-1 blockade. ELISPOT analysis from one representative experiment, demonstrating the frequency of MOG-specific IFN-γ–producing T cells at different concentrations of antigen for WT (a) and CD28-deficient animals (b). In the WT group, anti–PD-1–treated animals (solid bars) had a higher frequency of MOG-specific IFN-γ–producing T cells at all antigen concentrations compared with controls (hatched bars, *, P = 0.017 by one-way ANOVA). In the CD28-deficient mice, a significant difference was also seen at higher antigen concentrations (*, P = 0.0254 by one-way ANOVA). (c) DTH measurement assessed by an increase in footpad skin thickness after intradermal injection with 50 μg antigen. DTH response was significantly greater in the anti–PD-1–treated animals than controls (*, P = 0.0245 by two-tailed Mann-Whitney U test). (d) Serum level of anti-MOG antibodies obtained on day 14 after immunization were greater in anti–PD-1–treated animals than controls in both WT and CD28-deficient animals (*, P = 0.0476; **, P = 0.0009 by two-tailed Mann-Whitney U test).

Histology of Spinal Cords from Anti–PD-1–treated Animals and Controls. Histological examination of spinal cord sections from mice treated with anti–PD-1 or control IgG on day 14 after immunization mirrored the clinical course (Fig. 4). Compared with the control mice, both WT and CD28-deficient mice treated with anti–PD-1 mAb exhibited increased cellular infiltration into the CNS of $CD4^+$ and $CD8^+$ lymphocytes and $F4/80^+$ macrophages. Interestingly, there was an excess of $CD8^+$ cells in the CNS of mice treated with anti–PD-1 mAb, suggesting that the PD-1 pathway preferentially regulates encephalitogenic $CD8^+$ cells, in keeping with previous reports demonstrating greater sensitivity of $CD8^+$ cells to PD-1–mediated suppression (12).

The Effect of PD-1 Blockade on OVA-specific T Cell Responses. Because ELISPOT frequencies of MOG-reactive IFN-γ–producing T cells were increased after PD-1 blockade in normal and CD28-deficient mice, we decided to examine the effect of PD-1 blockade on T cell expansion and production of Th1/Th2 cytokines using another antigen-specific system. We used the adoptive transfer of OVA-specific T cells from DO11.10 TCR transgenic mice (6, 19, 20). Naive BALB/c mice were adoptively transferred with DO11.10 splenocytes and their responses after

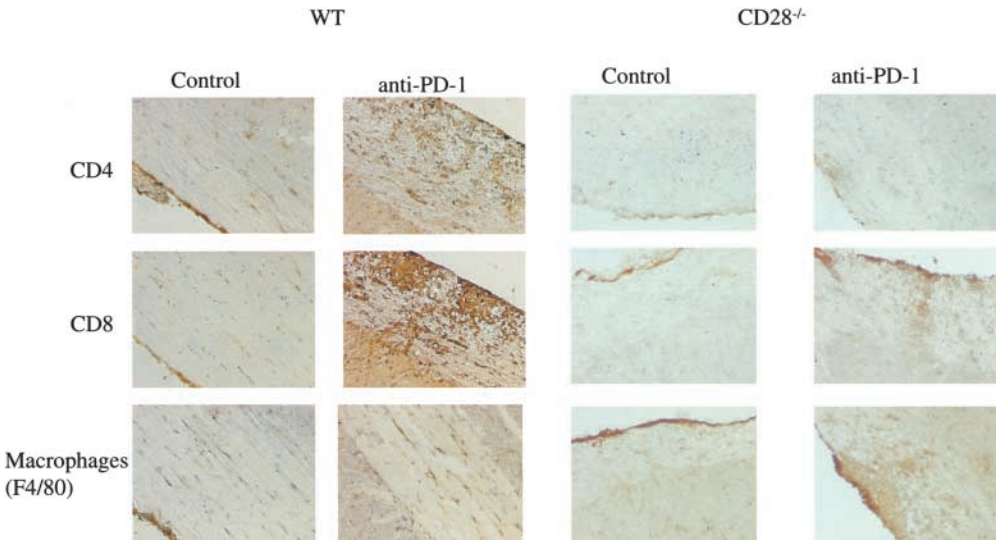

Figure 4. Immunohistology of the CNS in animals treated with PD-1 blockade. Spinal cord sections from WT and CD28-deficient animals treated with anti–PD-1 or control antibody were obtained on day 14 after immunization and stained with anti-CD4, anti-CD8, and anti-F4/80. There is a visible increase in the number of $CD4^+$ and $CD8^+$ T cells as well as the macrophages ($F4/80^+$ cells) in the anti–PD-1–treated mice, compared with controls in both the WT and CD28-deficient animals, more apparent in the former (×200).

immunization with OVA peptide and treatment with anti–PD-1 mAb or control IgG were examined. The transferred DO11.10 T cells were identified by using an anti-TCR clonotypic mAb KJ1-26 (Fig. 5, a and b). Control nonimmunized mice demonstrated that the $CD4^+$ $KJ1\text{-}26^+$ DO11.10 T cells made up <0.7% of the lymph node cells (corresponding to a total of 1.6×10^3 $CD4^+$ $KJ1\text{-}26^+$ cells; not depicted). However, after immunization with OVA peptide, there was a significant expansion of antigen-specific T cells in the draining lymph nodes. In the control IgG–treated animals this reached $5.7 \pm 0.6 \times 10^6$ cells, whereas in the anti–PD-1–treated animals this reached $91.8 \pm 20.9 \times 10^6$, reflecting a marked (16-fold) expansion of antigen-specific T cells (Fig. 5 c; $P < 0.0001$). Furthermore, a greater percentage of cells expressed the activation marker CD25 (94.3 ± 2.2% compared with 76.8 ± 8.9% in anti–PD-1–treated and control mice, respectively). Finally, PD-1 blockade resulted in a greater number of cells producing both Th1 (IFN-γ: $16.7 \pm 0.8 \times 10^5$ vs. $5.7 \pm 0.13 \times 10^5$, anti–PD-1 and control, respectively) and Th2 (IL-4: $46.49 \pm 7.08 \times 10^5$ vs. $4.98 \pm 1.46 \times 10^5$; IL-5: $32.37 \pm 17.9 \times 10^5$ vs. 0; and IL-10: $6.25 \pm 3.4 \times 10^5$ vs. 0) cytokines (not depicted).

Discussion

The outcome of T cell responses to their cognate antigens is dependent on the balance between activating and inhibitory signals (5, 23). PD-1 is a newly described member of the CD28/CTLA-4 superfamily, which acts as a negative regulator of activated T cells (8, 10, 16). PD-1–deficient mice develop splenomegaly and autoimmunity in the form of arthritis, nephritis, or cardiomyopathy, the phenotype being dependent on their genetic background (13, 14). Therefore, it has been suggested that the PD-1 pathway may serve as an important regulator of peripheral tolerance (16). In this report we demonstrated that the PD-1 pathway serves to regulate the autoimmune, MOG-reactive T cells in EAE. After PD-1 blockade a classical pattern of EAE disease developed (with ascending paralysis), but this was of greater severity than in control mice. In particular, this pathway appears to inhibit a population of CNS-infiltrating T cells, which were minimally present in cord sections of control EAE mice, but were more prominent in those from anti–PD-1–treated animals. Furthermore, PD-1 blockade was associated with increased frequencies of autoreactive (MOG-specific) T cells, increased DTH responses to the autoantigen, and greater autoantibody production. Finally, based on the anti-OVA response data, it appears that the PD-1 pathway inhibits not only antigen-specific T cell expansion, but also T cell activation and the production of both Th1 and Th2 cytokines. It is therefore not surprising that after PD-1 pathway blockade, EAE was augmented. Interestingly, this occurred in both WT and CD28-deficient animals, the latter normally being resistant to disease induction, after a single immunization with MOG (3, 22). We previously demonstrated that CTLA-4 blockade in CD28-deficient animals resulted in mild to modest disease induction (3), although the mean maximum disease score reached after CTLA-4 blockade was lower than that after PD-1 blockade. CD28-deficient T cells remain capable of up-regulating PD-1 after activation (not depicted), and together these data suggest that in the absence of CD28 signaling, T cell activation is largely kept in check by the PD-1 inhibitory pathway, as well as by the CTLA-4 pathway. This is also in keeping with recently published data demonstrating a greater inhibitory effect of the PD-1 pathway on T cells activated through the ICOS rather than CD28 costimulatory pathway (24). Interestingly, delayed PD-1 blockade had no effect on disease severity in WT mice, suggesting that once primed, effector T cells are less susceptible to inhibitory PD-1 signals. However, our model is one of progressive disease and the role of PD-1 on effector T cells and maintenance of tolerance may best be demonstrated in a relapsing-remitting disease model (25), as has been shown for CTLA-4 (25, 26).

PD-L1 is expressed not only on haemopoietic APCs but also on parenchymal cells, such as cardiac myocytes, renal

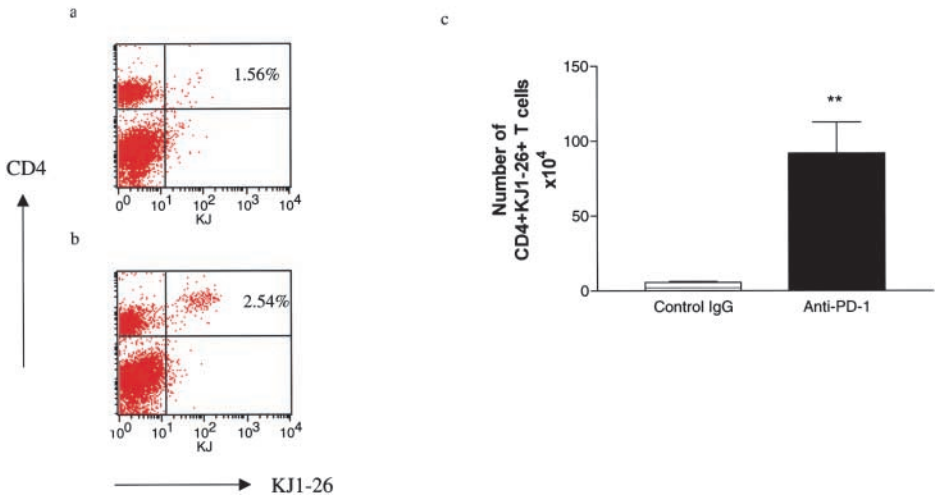

Figure 5. Effect of PD-1 blockade on antigen-specific cells in vivo. DO11.10 TCR Tg cells (3×10^6 cells per mouse) were transferred into BALB/c mice. 4 d after priming with OVA peptide, the draining lymph nodes were collected and the number of OVA-specific ($KJ1\text{-}26^+$) $CD4^+$ T cells was measured. (a) Flow cytometry plot of $CD4^+$ $KJ1\text{-}26^+$ cells from control IgG–treated animals, demonstrating that 1.54% of lymph node cells were TCR transgenic $CD4^+$ T cells. (b) By comparison, in the anti–PD1–treated animal 2.5% of lymph node cells were TCR transgenic. (c) Calculating the absolute numbers of TCR transgenic cells demonstrates a significant increase in $KJ1\text{-}26^+$ $CD4^+$ T cells in the anti–PD-1–treated animals compared with controls ($P < 0.0001$ by two-tailed Mann-Whitney U test).

tubular cells, and microvascular endothelial cells as well as cancer cell lines (11, 27, 28). By contrast, PD-L2 has more limited expression, predominantly on cytokine-activated macrophages and dendritic cells (11, 18). These patterns of expression may allow for the termination of an immune response in inflamed tissues, limiting organ damage, or in tumors allowing for immune evasion (27). We have found abundant expression of PD-L1 but minimal PD-L2 expression in the brains of animals with EAE. Moreover, we demonstrated only PD-L1 expression on resident brain cells. However, our in vivo data demonstrate that PD-L2 and not PD-L1 blockade augments disease, suggesting that the PD-1–mediated regulation might be occurring in the peripheral lymphoid organs and not within the brain itself. Further confirmation of this hypothesis will require the generation of bone marrow chimeras from WT and PD-1L–deficient animals, which is part of ongoing work. Alternatively, there remains the remote possibility that the anti–PD-L2 mAb might be providing a "positive" signal to dendritic cells, enhancing their immunostimulatory abilities, as has been demonstrated for certain IgM antibodies (29). Interestingly, these findings are in contrast to those in the NOD diabetes model (19), in which PD-1 and PD-L1 but not PD-L2 blockade precipitated disease and insulitis. The disparate effects in these models may reflect differences between spontaneous and induced autoimmune diseases. Notably, they are reminiscent of the disparate effects of B7-1 versus B7-2 blockade in EAE and autoimmune diabetes (30, 31).

Although the autoimmune phenotype of the PD-1–deficient mice as well as other in vitro data suggest that the PD-1 pathway is inhibitory (13, 14), conflicting data as to its role exist. Some reports have suggested that PD-L1 can enhance T cell proliferation and IL-10 production (9), and PD-L2 can promote proliferation of naive T cells and Th1 cytokine production (32). Moreover, ligation of PD-L1 may costimulate T cells (33) and ligation of PD-L2 by cross-linking IgM antibodies may activate dendritic cells and augment T cell responses (29). Thus, an alternative explanation for our findings might be that the antibodies used could be stimulatory in vivo. However, several pieces of evidence indicate that the IgG antibodies used in our experiments do not appear to be mediating their effects by stimulating T cell responses. In vivo, Fab fragments of anti–PD-1 mAb (J43) augment immune responses to the same extent as the whole antibody (unpublished data) and in vitro, the anti–PD-L1 (MIH6) and anti–PD-L2 (TY25) whole antibodies and Fab fragments block the suppression of proliferative responses of preactivated T cells by PD-L1 and PD-L2 transfectants, respectively (unpublished data). Moreover, the disparate effects of anti–PD-L1 and anti–PD-L2 mAbs in EAE and NOD diabetes (19) argue against the antibodies acting agonistically.

In conclusion, our data demonstrate an important role for immune regulation by PD-1 in EAE, an induced autoimmune disease. The challenge now is to manipulate this pathway therapeutically and allow termination of ongoing autoimmune reactions by stimulating the PD-1 pathway. Indeed, a recent report using a PD-L1 fusion protein in the context of an alloimmune response demonstrated that such a strategy is feasible and beneficial (34).

We are grateful to Talia Alexa Natori for providing technical assistance.

This work is supported by grants RG2988B6 from the National Multiple Sclerosis Society, and AI43496, AI40945, and AI46130 from NIH. A.D. Salama is a recipient of a Peel Medical Trust Award and a travelling fellowship from the British Renal Association. T. Chitnis is funded by the Nancy Davis Center Without Walls.

Submitted: 11 December 2002
Revised: 24 April 2003
Accepted: 2 May 2003

References

1. Begolka, W.S., C.L. Vanderlugt, S.M. Rahbe, and S.D. Miller. 1998. Differential expression of inflammatory cytokines parallels progression of central nervous system pathology in two clinically distinct models of multiple sclerosis. *J. Immunol.* 161:4437–4446.
2. Miller, S.D., C.L. Vanderlugt, D.J. Lenschow, J.G. Pope, N.J. Karandikar, M.C. Dal Canto, and J.A. Bluestone. 1995. Blockade of CD28/B7-1 interaction prevents epitope spreading and clinical relapses of murine EAE. *Immunity*. 3: 739–745.
3. Chitnis, T., N. Najafian, K.A. Abdallah, V. Dong, H. Yagita, M.H. Sayegh, and S.J. Khoury. 2001. CD28-independent induction of experimental autoimmune encephalomyelitis. *J. Clin. Invest.* 107:575–583.
4. Rottman, J.B., T. Smith, J.R. Tonra, K. Ganley, T. Bloom, R. Silva, B. Pierce, J.C. Gutierrez-Ramos, E. Ozkaynak, and A.J. Coyle. 2001. The costimulatory molecule ICOS plays an important role in the immunopathogenesis of EAE. *Nat. Immunol.* 2:605–611.
5. Van Parijs, L., and A.K. Abbas. 1998. Homeostasis and self-tolerance in the immune system: turning lymphocytes off. *Science*. 280:243–248.
6. Greenwald, R.J., V.A. Boussiotis, R.B. Lorsbach, A.K. Abbas, and A.H. Sharpe. 2001. CTLA-4 regulates induction of anergy in vivo. *Immunity*. 14:145–155.
7. Karandikar, N.J., C.L. Vanderlugt, T.L. Walunas, S.D. Miller, and J.A. Bluestone. 1996. CTLA-4: a negative regulator of autoimmune disease. *J. Exp. Med.* 184:783–788.
8. Agata, Y., A. Kawasaki, H. Nishimura, Y. Ishida, T. Tsubata, H. Yagita, and T. Honjo. 1996. Expression of the PD-1 antigen on the surface of stimulated mouse T and B lymphocytes. *Int. Immunol.* 8:765–772.
9. Dong, H., G. Zhu, K. Tamada, and L. Chen. 1999. B7-H1, a third member of the B7 family, co-stimulates T-cell proliferation and interleukin-10 secretion. *Nat. Med.* 5:1365–1369.
10. Freeman, G.J., A.J. Long, Y. Iwai, K. Bourque, T. Chernova, H. Nishimura, L.J. Fitz, N. Malenkovich, T. Okazaki, M.C. Byrne, et al. 2000. Engagement of the PD-1 immunoinhibitory receptor by a novel B7 family member leads to negative regulation of lymphocyte activation. *J. Exp. Med.* 192:1027–1034.
11. Latchman, Y., C.R. Wood, T. Chernova, D. Chaudhary, M. Borde, I. Chernova, Y. Iwai, A.J. Long, J.A. Brown, R.

Nunes, et al. 2001. PD-L2 is a second ligand for PD-1 and inhibits T cell activation. *Nat. Immunol.* 2:261–268.
12. Carter, L., L.A. Fouser, J. Jussif, L. Fitz, B. Deng, C.R. Wood, M. Collins, T. Honjo, G.J. Freeman, and B.M. Carreno. 2002. PD-1:PD-L inhibitory pathway affects both CD4(+) and CD8(+) T cells and is overcome by IL-2. *Eur. J. Immunol.* 32:634–643.
13. Nishimura, H., M. Nose, H. Hiai, N. Minato, and T. Honjo. 1999. Development of lupus-like autoimmune diseases by disruption of the PD-1 gene encoding an ITIM motif-carrying immunoreceptor. *Immunity.* 11:141–151.
14. Nishimura, H., T. Okazaki, Y. Tanaka, K. Nakatani, M. Hara, A. Matsumori, S. Sasayama, A. Mizoguchi, H. Hiai, N. Minato, et al. 2001. Autoimmune dilated cardiomyopathy in PD-1 receptor-deficient mice. *Science.* 291:319–322.
15. Tivol, E.A., F. Borriello, A.N. Schweitzer, W.P. Lynch, J.A. Bluestone, and A.H. Sharpe. 1995. Loss of CTLA-4 leads to massive lymphoproliferation and fatal multiorgan tissue destruction, revealing a critical negative regulatory role of CTLA-4. *Immunity.* 3:541–547.
16. Nishimura, H., and T. Honjo. 2001. PD-1: an inhibitory immunoreceptor involved in peripheral tolerance. *Trends Immunol.* 22:265–268.
17. Chitnis, T., N. Najafian, C. Benou, A.D. Salama, M.J. Grusby, M.H. Sayegh, and S.J. Khoury. 2001. Effect of targeted disruption of STAT4 and STAT6 on the induction of experimental autoimmune encephalomyelitis. *J. Clin. Invest.* 108:739–747.
18. Yamazaki, T., H. Akiba, H. Iwai, H. Matsuda, M. Aoki, Y. Tanno, T. Shin, H. Tsuchiya, D.M. Pardoll, K. Okumura, et al. 2002. Expression of programmed death 1 ligands by murine T cells and APC. *J. Immunol.* 169:5538–5545.
19. Ansari, M.J.I., A.D. Salama, R.N. Smith, H. Yagita, H. Akiba, M. Azuma, H. Iwai, S.J. Khoury, H. Auchincloss, and M.H. Sayegh. 2003. The Programmed Death 1 (PD-1) pathway regulates autoimmune diabetes in NOD mice. *J. Exp. Med.* 198:63–69.
20. Kearney, E.R., K.A. Pape, D.Y. Loh, and M.K. Jenkins. 1994. Visualization of peptide-specific T cell immunity and peripheral tolerance induction in vivo. *Immunity.* 1:327–339.
21. Issazadeh, S., M. Zhang, M.H. Sayegh, and S.J. Khoury. 1999. Acquired thymic tolerance: role of CTLA4 in the initiation and maintenance of tolerance in a clinically relevant autoimmune disease model. *J. Immunol.* 162:761–765.
22. Girvin, A.M., M.C. Dal Canto, L. Rhee, B. Salomon, A. Sharpe, J.A. Bluestone, and S.D. Miller. 2000. A critical role for B7/CD28 costimulation in experimental autoimmune encephalomyelitis: a comparative study using costimulatory molecule-deficient mice and monoclonal antibody blockade. *J. Immunol.* 164:136–143.
23. Ravetch, J.V., and L.L. Lanier. 2000. Immune inhibitory receptors. *Science.* 290:84–89.
24. Bennett, F., D. Luxenberg, V. Ling, I.M. Wang, K. Marquette, D. Lowe, N. Khan, G. Veldman, K.A. Jacobs, V.E. Valge-Archer, et al. 2003. Program Death-1 engagement upon TCR activation has distinct effects on costimulation and cytokine-driven proliferation: attenuation of ICOS, IL-4, and IL-21, but not CD28, IL-7, and IL-15 responses. *J. Immunol.* 170:711–718.
25. Issazadeh, S., V. Navikas, M. Schaub, M. Sayegh, and S. Khoury. 1998. Kinetics of expression of costimulatory molecules and their ligands in murine relapsing experimental autoimmune encephalomyelitis in vivo. *J. Immunol.* 161:1104–1112.
26. Karandikar, N.J., T.N. Eagar, C.L. Vanderlugt, J.A. Bluestone, and S.D. Miller. 2000. CTLA-4 downregulates epitope spreading and mediates remission in relapsing experimental autoimmune encephalomyelitis. *J. Neuroimmunol.* 109:173–180.
27. Dong, H., S.E. Strome, D.R. Salomao, H. Tamura, F. Hirano, D.B. Flies, P.C. Roche, J. Lu, G. Zhu, K. Tamada, et al. 2002. Tumor-associated B7-H1 promotes T-cell apoptosis: a potential mechanism of immune evasion. *Nat. Med.* 8:793–800.
28. Eppihimer, M.J., J. Gunn, G.J. Freeman, E.A. Greenfield, T. Chernova, J. Erickson, and J.P. Leonard. 2002. Expression and regulation of the PD-L1 immunoinhibitory molecule on microvascular endothelial cells. *Microcirculation.* 9:133–145.
29. Nguyen, L.T., S. Radhakrishnan, B. Ciric, K. Tamada, T. Shin, D.M. Pardoll, L. Chen, M. Rodriguez, and L.R. Pease. 2002. Cross-linking the B7 family molecule B7-DC directly activates immune functions of dendritic cells. *J. Exp. Med.* 196:1393–1398.
30. Kuchroo, V.K., M. Prabhu Das, J.A. Brown, A.M. Ranger, S.S. Zamvil, R.A. Sobel, H.L. Weiner, N. Nabavi, and L.H. Glimcher. 1995. B7-1 and B7-2 costimulatory molecules activate differentially the Th1/Th2 developmental pathways: application to autoimmune disease therapy. *Cell.* 80:707–718.
31. Lenschow, D.J., S.C. Ho, H. Sattar, L. Rhee, G. Gray, N. Nabavi, K.C. Herold, and J.A. Bluestone. 1995. Differential effects of anti–B7-1 and anti–B7-2 monoclonal antibody treatment on the development of diabetes in the nonobese diabetic mouse. *J. Exp. Med.* 181:1145–1155.
32. Tseng, S.Y., M. Otsuji, K. Gorski, X. Huang, J.E. Slansky, S.I. Pai, A. Shalabi, T. Shin, D.M. Pardoll, and H. Tsuchiya. 2001. B7-DC, a new dendritic cell molecule with potent costimulatory properties for T cells. *J. Exp. Med.* 193:839–846.
33. Dong, H., S.E. Strome, E.L. Matteson, K.E. Moder, D.B. Flies, G. Zhu, H. Tamura, C.L.W. Driscoll, and L. Chen. 2003. Costimulating aberrant T cell responses by B7-H1 autoantibodies in rheumatoid arthritis. *J. Clin. Invest.* 111:363–370.
34. Ozkaynak, E., L. Wang, A. Goodearl, K. McDonald, S. Qin, T. O'Keefe, T. Duong, T. Smith, J.C. Gutierrez-Ramos, J.B. Rottman, et al. 2002. Programmed death-1 targeting can promote allograft survival. *J. Immunol.* 169:6546–6553.